



## Probing vibrational modes in silica glass using inelastic neutron scattering with mass contrast

Richard Haworth,<sup>1</sup> Gavin Mountjoy,<sup>1</sup> Marta Corno,<sup>2</sup> Piero Ugliengo,<sup>2</sup> and Robert J. Newport<sup>1</sup>

<sup>1</sup>*School of Physical Sciences, University of Kent, Canterbury, Kent CT2 7NH, United Kingdom*

<sup>2</sup>*Dipartimento di Chimica IFM and Nanostructured Interfaces and Surfaces Centre of Excellence, Università degli Studi di Torino, Via P. Giuria 7, 10125 Torino, Italy*

(Received 21 January 2010; published 22 February 2010)

The effective vibrational density of states (VDOS) has been derived from inelastic neutron-scattering data, for isotopically substituted Si <sup>18</sup>O<sub>2</sub> and Si <sup>16</sup>O<sub>2</sub> glasses, to gain information about the relative contribution to the Si and O partial VDOS. This is a necessary point of comparison for vibrational mode analyses of molecular-dynamics models. The mass contrast has led to a measurable shift between vibrational mode frequencies in the effective VDOS of Si <sup>18</sup>O<sub>2</sub> and Si <sup>16</sup>O<sub>2</sub>, which is well reproduced in an *ab initio* simulation. The vibrational band centered at 100.2 meV is confirmed to have significantly lower contribution from the oxygen partial VDOS, than the higher (150.3 and 135.8 meV) and lower energy bands (53.3 meV).

DOI: [10.1103/PhysRevB.81.060301](https://doi.org/10.1103/PhysRevB.81.060301)

PACS number(s): 63.50.Lm, 61.05.fg, 61.43.Bn

Glasses remain challenging materials to study and understand due to the lack of long-range order in the structure. This is especially challenging in the case of vibrational modes, which in crystals are identified on the basis of symmetries present in the structure. Silica glass is fundamentally viewed as a prototype strong glass former, and archetypal model of the disordered network, as well as playing a key role in optical and electronic devices.

There have been many experimental studies<sup>1–6</sup> into the vibrational modes of silica glass, and several computational models explored.<sup>7–13</sup> Information about vibrations is available from the common techniques of IR and Raman spectroscopy, however, the visibility of modes is strongly dependent on complicated cross sections. An alternative experimental method is inelastic neutron scattering (INS), in which vibrations are probed by energy exchanges with thermal neutrons. While INS is more costly and time consuming compared to optical scattering methods, it provides an experimental route to a close approximation to the *true* vibrational density of states (VDOS),

$$g(\omega) = \frac{1}{3N} \sum_{j=1}^{3N} \delta(\omega - \omega_j) \quad (1)$$

where  $\omega_j$  are the characteristic frequencies of the vibrational modes in a system of  $N$  atoms. There have only been two previous INS experiments on silica glass which measured the complete VDOS.<sup>5,6</sup>

In an effort to realize more definitive information about vibrational modes in glasses, isotopes have been used. The use of isotopic substitution provides a *mass contrast*, resulting in a shift in frequency of the vibrational modes associated with a specific element (at the simplest level  $\omega = (k/\mu)^{1/2}$  where  $k$  is a force constant and  $\mu$  is the reduced mass). This provides a way to distinguish the contributions to vibrational modes from different elements and so allows a vital increase in the detail of information available for a proper mode analysis of vibrational spectra.

The dependence on the vibrational spectra of SiO<sub>2</sub> and B<sub>2</sub>O<sub>3</sub> glasses on isotopic mass has been investigated by Raman measurements by Galeener *et al.*<sup>3,4</sup> and Windisch *et al.*<sup>14</sup>

However, in Raman spectra vibrational modes are weighted according to the change in polarizability which occurs, and this is difficult to simulate accurately. For this reason, modeling studies of vibrations in SiO<sub>2</sub> glass (e.g. Refs. 10–13) are not compared to experimental Raman spectra. Furthermore, the sample preparation method used in Ref. 3 could only produce thin films of material, and the method employed in Ref. 14 could not be applied to silica due to its higher melting temperature. So these earlier studies did not provide a way to obtain the larger amounts of SiO<sub>2</sub> glass needed for INS experiments.

Presented in this Rapid Communication is the comparison of the effective VDOS of vitreous Si <sup>16</sup>O<sub>2</sub> and Si <sup>18</sup>O<sub>2</sub> measured by inelastic neutron scattering. Neutron-scattering experiments have long exploited the difference in scattering length of certain stable isotopes in order to increase information about static structure, referred to as *scattering length contrast*. However, the <sup>16</sup>O and <sup>18</sup>O isotopes have no significant difference in scattering length. In this case a glass has been studied with inelastic neutron scattering using mass contrast. The shifts in frequencies of the main features of the effective VDOS, between the natural and isotopically substituted systems, are compared with the VDOS calculated from *ab initio* B3LYP simulations of Si <sup>16</sup>O<sub>2</sub> and Si <sup>18</sup>O<sub>2</sub> glasses and are discussed in light of recent mode analyses found in the literature.

A challenge for the work was to produce enough Si <sup>18</sup>O<sub>2</sub> in order to obtain the effective VDOS from a time-of-flight neutron-scattering experiment. This could not be done using melt quenching because <sup>18</sup>O available as H<sub>2</sub>O is not suitable, and <sup>18</sup>O available as oxide could not be melted at 1800 °C without risking exchange with <sup>16</sup>O in the atmosphere. The sample was prepared by the sol-gel technique described fully in reference 15, in which tetraethylorthosilicate (TEOS) is hydrolyzed in water, with hydrochloric acid acting as the catalyst, and gelled into a tetrahedrally coordinated silica-containing network. The gel is aged, dried, and then heat treated to condense the network further and remove organic compounds. The <sup>18</sup>O (in 98% + <sup>18</sup>O enriched water, from Rotem Industries) was introduced into the network during the initial hydrolysis stage, during the nucleophilic attack of the oxygen in water on the silicon atom in the TEOS precursor,

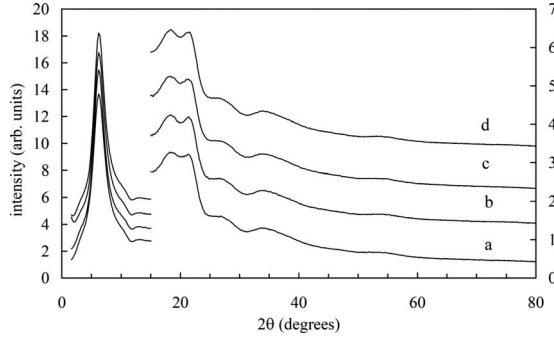
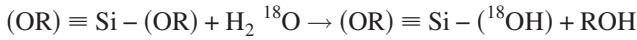


FIG. 1. High-energy synchrotron x-ray diffraction ( $\lambda = 0.486 \text{ \AA}$ ), performed on station 9.1 at Daresbury SRS, U.K.  $\text{SiO}_2$  glass prepared by (a) melt quenching, (b) sol-gel method in air, (c) sol-gel method in  $\text{N}_2$ , and (d)  $\text{Si}^{18}\text{O}_2$  glass prepared by sol-gel method in  $\text{N}_2$ .



where OR represents the alkoxy group. The process was carried out entirely under “zero-grade” nitrogen (BOC Gases), as was the subsequent aging, drying and heat treating, to eliminate the possible exchange of  $^{18}\text{O}$  with other isotopes in the atmosphere.<sup>14</sup> An  $\text{Si}^{16}\text{O}_2$  sample was produced under identical conditions with distilled water containing natural oxygen (99.76%  $^{16}\text{O}$ ). Both samples were stored under a nitrogen atmosphere. Figure 1 shows high-energy synchrotron x-ray diffraction ( $\lambda = 0.486 \text{ \AA}$ ), performed on station 9.1 at Daresbury SRS, U.K. The static structure factor of the sol-gel produced glasses is the same as that of silica glass produced by the melt-quench method (Sigma-Aldrich 342831).

The inelastic neutron-scattering data was measured, for 15 g of both  $\text{Si}^{16}\text{O}_2$  and  $\text{Si}^{18}\text{O}_2$ , with the MARI instrument at the ISIS spallation neutron source in the Rutherford Appleton Laboratory, U.K. The samples were shaped with an annular geometry to reduce multiple-scattering events. The MARI R chopper frequency was 450 Hz and the incident neutron energy was 230 meV. These details are required for the application of the instrumental resolution to model data. The multiple scattering was calculated from the reduced data and subtracted before deriving the one-phonon generalized vibrational density of states,  $G(Q, \omega)$ , as a function of the scattering vector magnitude,  $Q$ , and the vibrational frequency,  $\omega$ . In the incoherent approximation (e.g., see Refs. 5 and 16),

$$G(Q, \omega) = B(Q, \omega)S(Q, \omega) \quad (2)$$

where the dynamical structure factor  $S(Q, \omega)$  is obtained directly from the INS experiment in a single measurement, and

$$B(Q, \omega) = \frac{2\bar{M}}{\hbar Q^2} e^{2\bar{W}} [n(\omega) + 1]^{-1} \quad (3)$$

corrects for the scattering dependence on the average atomic mass  $\bar{M}$ , the average of the Debye-Waller factors over all atoms in the sample  $\bar{W}$ , and the thermal-equilibrium averaged occupation number  $n(\omega) = [\exp(\hbar\omega/kT) - 1]^{-1}$ . The

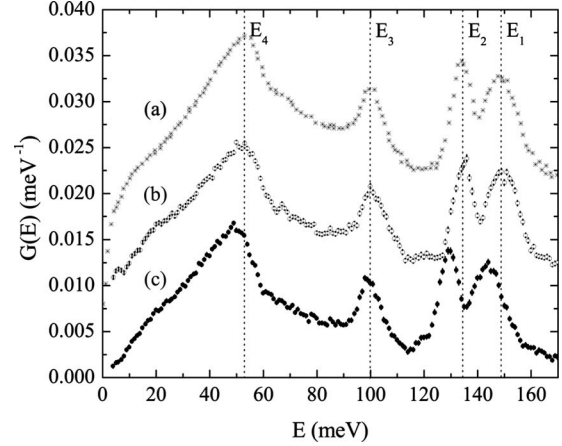


FIG. 2. Effective VDOS,  $G(E)$ , for (a)  $\text{Si}^{16}\text{O}_2$  as measured by Arai *et al.*, and (b)  $\text{Si}^{16}\text{O}_2$  and (c)  $\text{Si}^{18}\text{O}_2$  measured for this study. Error bars are included, and are comparable to the symbol size. The data of Arai *et al.* have been digitized from Ref. 6.

value of  $\bar{W}$  used was obtained from Ref. 17, and the effect of  $n(\omega)$  was reduced by maintaining the sample at a very low temperature (5 K) during the experiment.

In order to remove the  $Q$  dependence of  $G(Q, \omega)$ , it is integrated and averaged over  $Q$  in the largest range ( $5 < Q < 16 \text{ \AA}^{-1}$ ) available from the experimental configuration.<sup>5</sup> The resulting *effective* VDOS  $G(\omega)$  is closely related to the true VDOS defined in Eq. (1) by a correction function  $C(\omega) \approx 1$  such that

$$G(\omega) = C(\omega)g(\omega) \quad (4)$$

$C(\omega)$  has been calculated not to differ from unity by more than 20%.<sup>18</sup>

In Fig. 2  $G(\omega)$  is presented as a function of energy, i.e.,  $G(E)$  where  $E = \hbar\omega$ , for the  $\text{Si}^{18}\text{O}_2$  and  $\text{Si}^{16}\text{O}_2$  glasses and is compared to the previously measured  $G(E)$  for silica glass ( $\text{Si}^{16}\text{O}_2$ ) by Arai *et al.*<sup>6</sup> Another previous measurement by Price *et al.* is of lower resolution.<sup>5</sup> The effective VDOS of our  $\text{Si}^{16}\text{O}_2$  sample is in excellent agreement with Arai’s measurement. This comparison highlights the significant differences observed in the four main band positions in the  $G(E)$  of  $\text{Si}^{18}\text{O}_2$  compared to the  $G(E)$  of  $\text{Si}^{16}\text{O}_2$ .

Table I lists band center positions  $E_1$ - $E_4$  shown in Fig. 2 (centered at 150.3, 135.8, 102.2, and 53.3 meV, respectively, for the  $\text{Si}^{16}\text{O}_2$  samples) and absolute and relative shifts between the  $\text{Si}^{16}\text{O}_2$  and  $\text{Si}^{18}\text{O}_2$  measurements. The bands were fitted with asymmetric Gaussian functions, of which the centers of gravity define the band centers. The absolute shifts in energy are largest for the two high-energy bands ( $E_1$  and  $E_2$ ), and smallest for the 102.2 meV band ( $E_3$ ). The shifts are not symmetric around the band centers.

The *ab initio* results were obtained in the following way. The simulated  $\text{SiO}_2$  glass utilizes an amorphous 72-atom supercell, relaxed at density-functional-theory level by Bakos *et al.*,<sup>19</sup> as an initial starting structure. Using the CRYSTAL06 code,<sup>20</sup> the structure was optimized at the B3LYP level,<sup>21,22</sup> a commonly used procedure in the *ab initio* simulation of glasses which effectively enables only short-range relax-

TABLE I. Band center energies for the two silica samples and their absolute and relative shifts. All measurements are in meV (apart from %) with an uncertainty in the center positions of  $\pm 0.2$  meV.

Band	$E_1$	$E_2$	$E_3$	$E_4$
Expt.				
Si $^{16}\text{O}_2$	150.3	135.8	102.2	53.3
Si $^{18}\text{O}_2$	144.6	130.3	100.7	50.1
Abs. shift	5.7	5.6	1.6	3.2
Rel. shift	3.8%	4.1%	1.5%	5.9%
<i>Ab initio</i>				
Si $^{16}\text{O}_2$	143.6	129.4	102.2	44.2
Si $^{18}\text{O}_2$	137.8	124.3	100.8	47.8
Abs. shift	5.8	5.1	1.3	2.4
Rel. shift	4.0%	4.0%	1.3%	5.5%

ations. The B3LYP functional has good performance in predicting IR and Raman spectra of oxides.<sup>22</sup> A full description of the procedure and computational parameters can be found in Ref. 23. A mass-weighted Hessian matrix was obtained by numerical differentiation of the analytical first derivative of the electronic and nuclear repulsion energy, calculated at geometries obtained by small displacements of each of the  $3N$  nuclear coordinates with respect to their equilibrium positions. Values of  $\omega_j$  have been calculated as the eigenvalues found from diagonalizing the dynamical matrix associated with the  $\Gamma$  point, a complete discussion of which can be found in Ref. 24.

In the case of vitreous silica, most previously published comparisons of experimental and simulated VDOS disregard the real instrumental broadening in favor of an arbitrary function. The instrument resolution, calculated using the MCHOP program,<sup>25</sup> is shown in Fig. 3, and has been used to broaden the calculated  $\omega_j$  values. The *ab initio* results are

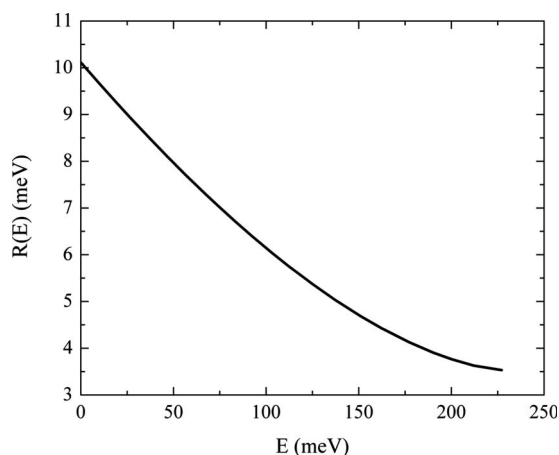


FIG. 3. Instrument resolution function  $R(e)$  calculated using the MCHOP program (Ref. 25) for the MARI R chopper package with frequency of 450 Hz and incident neutron energy of 230 meV.

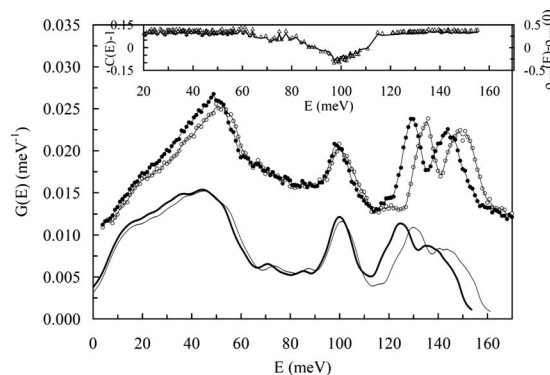


FIG. 4. Effective VDOS,  $G(E)$ , derived from (a) experimental data for Si  $^{16}\text{O}_2$  (open circles) and Si  $^{18}\text{O}_2$  (closed circles), and (b) *ab initio* results for Si  $^{16}\text{O}_2$  (lightly weighted line) and Si  $^{18}\text{O}_2$  (heavily weighted line). The inset shows (triangles) the correction function  $C(\omega)-1$  [see Eq. (4)] and (solid line) the oxygen partial VDOS  $\rho_{\text{oxy}}(E)-\rho_{\text{oxy}}(0)$  [see Eq. (5)] from the *ab initio* results.

shown in Fig. 4 and reproduce reasonably accurately the key features in the experimental effective vibrational density of states. In particular, the four main band center positions (see Table I), and their relative intensities show a good similarity. Figure 4 inset shows the value of  $C(E)-1$  calculated from the *ab initio* results, and as shown previously<sup>18</sup> the effective VDOS has more intense  $E_1$ ,  $E_2$ , and  $E_4$  bands because  $C(\omega) > 1$  [see Eq. (4)]. The main deficiency of the *ab initio* results is that the highest frequency bands at 150.3 and 135.8 meV appear at slightly lower frequency. This is a known weakness of the B3LYP and other generalized gradient approximation functionals, resulting from the overestimation of the Si-O bond lengths.<sup>26,27</sup> The effect of  $^{18}\text{O}$  mass contrast on the *ab initio* results (see Fig. 4 and Table I) is seen to show a remarkable similarity to the experimental effect of  $^{18}\text{O}$  mass contrast.

Recent studies<sup>10-13</sup> using classical and first principle molecular-dynamics (MD) models mostly concentrate the mode analysis on the local vibrations associated with the  $\text{SiO}_4$  tetrahedral units and O-Si-O and Si-O-Si three-body units in the model. All agree that the origins of the 150.3 and 135.8 meV bands are mainly from the symmetric and asymmetric stretches of  $\text{SiO}_4$  units, with the symmetric stretch contributing mostly to the upper of these bands<sup>10-13</sup> and that it is the partial VDOS of oxygen atoms that dominates.<sup>11,13</sup> In these bands we see the largest shifts between the  $G(E)$  of Si  $^{18}\text{O}_2$  and Si  $^{16}\text{O}_2$  which is in excellent agreement with the relative shifts from the two *ab initio* models of these systems (see  $E_1$  and  $E_2$ , Table I). The similarity of the size of the shifts for these two high-energy bands support models assigning the doublet to local modes with similar contributions to the oxygen partial VDOS.

Mode analysis of MD models has also suggested the origin of the feature at 100.2 meV ( $E_3$ ); it corresponds to a mixture of  $\text{SiO}_4$  stretching and  $\text{SiO}_4$  bending modes,<sup>10,11</sup> where the motion relative to Si-O-Si units is mostly bending.<sup>11,13</sup> The results from MD models show this feature to have the largest contribution from the partial VDOS of silicon atoms.<sup>11,13</sup> The relative partial VDOS for oxygen is<sup>18</sup>



$$\rho_{\text{oxy}}(\omega) = g_{\text{oxy}}(\omega)/g(\omega). \quad (5)$$

Figure 4 inset shows  $\rho_{\text{oxy}}(E) - \rho_{\text{oxy}}(0)$  [see Eqs. 23 and 25 of Ref. 18] from the *ab initio* results, and this is lowest for the feature  $E_3$ . This is consistent with experimental results, which show the feature  $E_3$  has the smallest shift due to  $^{18}\text{O}$  mass contrast. Hence, we have direct experimental confirmation of the relative participation of Si and O atoms in this vibrational band, as predicted from mode analysis of MD models. Furthermore, an asymmetry of this band shift is observed in both the INS and *ab initio* results. Modes on the higher energy side undergo a larger shift than those on the lower energy side resulting in a 10% and 8% reduction in the FWHM of the band in INS and *ab initio* results, respectively. This effect must originate from an unequal relative distribution of (a) oxygen-associated bending and stretching modes, and/or (b) the oxygen and silicon partial VDOS. Moreover, the oxygen partial VDOS must shift from higher energies, toward the band center,  $E_3$ . This asymmetry of band shift is not observed in the two upper bands,  $E_1$  and  $E_2$ , which is probably because they are dominated by the oxygen partial VDOS, and a single type of mode (stretching).

The fourth prominent feature in the  $G(E)$ , which we have also highlighted in Table I, is the large band of intensity centered around 53.3 meV ( $E_4$ ). A systematic shift due to  $^{18}\text{O}$  mass contrast is apparent in the high-energy edge of this feature, in both experimental and *ab initio* data, around 53–60 meV. In MD modeling studies, the high-energy edge of this feature denotes where stretching modes no longer

make a major contribution. Wilson *et al.*<sup>10</sup> attributed this feature to  $\text{SiO}_4$  bending, while Sarnthien *et al.*<sup>12</sup> attributed it to Si-O-Si bending. The results of Taraskin *et al.*<sup>11</sup> also make these attributions and furthermore show that there is a major contribution from the partial VDOS of oxygen atoms, with silicon atoms making a smaller contribution. Our observed relative shifts are close to the maximum possible shift of 5.7% from  $\omega = (k/\mu)^{1/2}$  when only the oxygen is in motion.

In summary, we have found that synthesizing a sample of  $^{18}\text{O}$ -substituted  $\text{SiO}_2$  glass suitable for an inelastic neutron-scattering experiment is achievable through the sol-gel technique. The  $G(E)$  of  $\text{Si } ^{18}\text{O}_2$ , derived from INS experiments, show clear shifts in the vibrational modes to lower energies when compared to that of  $\text{Si } ^{16}\text{O}_2$ , in accordance with mass contrast. The shifts are well reproduced by a simulated *ab initio* model, emphasizing that the experimental data provides a vital point of comparison in a field which relies mainly on computational techniques. The results of MD models have been compared here (and should continue to be compared) with this data set. It is experimentally confirmed that the vibrational band centered at 100.2 meV has a lower oxygen partial VDOS contribution, in comparison to the higher energy bands which are dominated by the oxygen contribution.

This work was funded by EPSRC-GB (Grant No. EP/D06001X/1) and supported by beam-time allocation from the STFC. The authors would like to extend their thanks to MARI instrument scientist, J. W. Taylor.

- <sup>1</sup>J. M. Carpenter and D. L. Price, Phys. Rev. Lett. **54**, 441 (1985).
- <sup>2</sup>F. L. Galeener, A. J. Leadbetter, and M. W. Stringfellow, Phys. Rev. B **27**, 1052 (1983).
- <sup>3</sup>F. L. Galeener and J. C. Mikkelsen, Phys. Rev. B **23**, 5527 (1981).
- <sup>4</sup>F. L. Galeener and A. E. Geissberger, Phys. Rev. B **27**, 6199 (1983).
- <sup>5</sup>D. L. Price and J. M. Carpenter, J. Non-Cryst. Solids **92**, 153 (1987).
- <sup>6</sup>M. Arai, A. C. Hannon, A. D. Taylor, A. C. Wright, R. N. Sinclair, and D. L. Price, Physica B **180-181**, 779 (1992).
- <sup>7</sup>L. Giacomazzi, P. Umari, and A. Pasquarello, Phys. Rev. B **79**, 064202 (2009).
- <sup>8</sup>J. Burgin, C. Guillon, P. Langot, F. Vallee, B. Hehlen, and M. Foret, Phys. Rev. B **78**, 184203 (2008).
- <sup>9</sup>T. T. To, D. Bougeard, and K. S. Smirnov, J. Raman Spectrosc. **39**, 1869 (2008).
- <sup>10</sup>M. Wilson, P. A. Madden, M. Hemmati, and C. A. Angell, Phys. Rev. Lett. **77**, 4023 (1996).
- <sup>11</sup>S. N. Taraskin and S. R. Elliott, Phys. Rev. B **56**, 8605 (1997).
- <sup>12</sup>J. Sarnthien, A. Pasquarello, and R. Car, Science **275**, 1925 (1997).
- <sup>13</sup>A. Pasquarello, J. Sarnthien, and R. Car, Phys. Rev. B **57**, 14133 (1998).
- <sup>14</sup>C. F. Windisch, Jr. and W. M. Risen, Jr., J. Non-Cryst. Solids **48**, 325 (1982).
- <sup>15</sup>R. Anderson, G. Mountjoy, M. E. Smith, and R. J. Newport, J. Non-Cryst. Solids **232-234**, 72 (1998).
- <sup>16</sup>K. Sköld and D. L. Price, *Neutron Scattering (Part A)* (Academic Press, Orlando, 1986), Vol. 23, p. 1.
- <sup>17</sup>A. C. Hannon, M. Arai, R. N. Sinclair, and A. C. Wright, J. Non-Cryst. Solids **150**, 239 (1992).
- <sup>18</sup>S. N. Taraskin and S. R. Elliott, Phys. Rev. B **55**, 117 (1997).
- <sup>19</sup>T. Bakos, S. N. Rashkeev, and S. T. Pantelides, Phys. Rev. Lett. **88**, 055508 (2002).
- <sup>20</sup>R. Dovesi, V. R. Saunders, C. Roetti, R. Orlando, C. M. Zicovich-Wilson, F. Pascale, B. Civalleri, K. Doll, N. M. Harrison, I. J. Bush, Ph. D'Arco, and M. Llunell, *CRYSTAL06 User's Manual* (Università di Torino, Italy, 2006).
- <sup>21</sup>A. D. Becke, J. Chem. Phys. **98**, 5648 (1993).
- <sup>22</sup>C. T. Lee, W. T. Yang, and R. G. Parr, Phys. Rev. B **37**, 785 (1988); A. M. Ferrari, L. Valenzano, A. Meyer, R. Orlando, and R. Dovesi, J. Phys. Chem. A **113**, 11289 (2009).
- <sup>23</sup>M. Corno, A. Pedone, R. Dovesi, and P. Ugliengo, Chem. Mater. **20**, 5610 (2008).
- <sup>24</sup>F. Pascale, C. M. Zicovich-Wilson, F. L. Gejo, B. Civalleri, R. Orlando, and R. Dovesi, J. Comput. Chem. **25**, 888 (2004).
- <sup>25</sup>D. Champion, F. Akeroyd, P. Amin, T. Perring, and D. Whittaker, *Homer User Manual* (ISIS Pulsed Neutron Source, Harwell, U.K., 2008).
- <sup>26</sup>M. R. Bar and J. Sauer, Chem. Phys. Lett. **226**, 405 (1994).
- <sup>27</sup>M. Sierka and J. Sauer, *General Discussion Meeting on Solid State Chemistry-New Opportunities from Computer Simulations* (Royal Society of Chemistry, London, U.K., 1997), p. 41.